Earth and Planetary Science Letters 271 (2008) 63–74

Contents lists available at ScienceDirect

Earth and Planetary Science Letters

journal homepage: www.elsevier.com/locate/epsl

HP-UHP exhumation during slow continental subduction: Self-consistent thermodynamically and thermomechanically coupled model with application to the Western Alps

P. Yamato [a,b,*], E. Burov [a], P. Agard [a], L. Le Pourhiet [a], L. Jolivet [a]

[a] Laboratoire de Tectonique, Université Pierre et Marie Curie-Paris 6, CNRS, UCP, Case 129-4 place Jussieu 75252 Paris, France
[b] Now at Geosciences Rennes, UMR 6118 CNRS, Université de Rennes 1, Rennes, France

ARTICLE INFO

Article history:
Received 18 June 2007
Received in revised form 20 March 2008
Accepted 23 March 2008
Available online 9 April 2008

Editor: R.D. van der Hilst

Keywords:
Western Alps
HP-UHP rocks
exhumation processes
thermomechanical modeling
exhumation rates
rheology

ABSTRACT

The exhumation of ultra-high pressure (UHP) crustal material often occurs at the rear of sedimentary accretion wedges (e.g., Alps, Himalaya, Norway). However, the mechanisms of deep (>100 km) burial in slow (<1–2 cm yr^{-1}) continental collision zones, where thermal diffusion competes with advection, resulting in weak slabs and Rayleigh-Taylor instabilities, may be different from those inferred from common kinematic models that are more applicable to fast convergence. In this study, we provide a thermodynamically and thermomechanically consistent numerical model explaining the mechanisms of exhumation of continental material in slow convergence zones such as the well-studied Western Alps. The results of the experiments are compatible with topographic and structural observations, and with pressure and temperature estimates from metamorphic petrology studies. The reported bimodal exhumation rate of HP rocks, fast at the initial (>10 mm yr^{-1}) and slow at the later stage (<4 mm yr^{-1}), is also well reproduced. The presence of a double-layered continental crust in the subducting plate leads to self-localization of non-predefined crustal splitting zones at the level of the brittle-ductile transition, from which the low-density continental material is exhumed. We conclude that syn-convergent exhumation at the rear of the accretionary wedge is a transient process (~10 Myr) largely controlled by buoyancy forces in the depth interval of 100–35 km, and by erosion at shallower depths, without significant impact from slab break-off.

1. Introduction

Most subduction-related HP-UHP metamorphic continental rocks (Liou et al., 2004; e.g., Alps, Dabie-Sulu, Himalaya, Norway) occur in zones of intracontinental collision. Although the transition from oceanic to continental subduction seems to be a continuous phenomenon (e.g., Lallemand et al., 2005), introduction of lighter continental material in the subduction zone is the source of strong buoyancy contrasts largely responsible for their exhumation, as shown by several analogue and numerical modeling studies (e.g., Burov et al., 2001; Burov and Yamato, 2007; Chemenda et al., 1995).

Interesting points about this type of metamorphism include the fact that: (1) exhumed continental material appears to be buried beyond lithospheric depths (>100–150 km; e.g., Liou et al., 2004; Chopin, 1984; Green, 2005). (2) Continental exhumation processes are short-lived, lasting ~10 Myr (e.g., Guillot et al., 2007; Hacker, 2007) and burial/exhumation processes for continental material are thus transient. (3) Such exhumation generally involves only a small quantity of material, as suggested by the small surface exposures of most UHP terrains (e.g. <2000 km^2 in the internal crystalline massifs of the Western Alps, Fig. 1). These areas are almost invariably exhumed as lenses of highly metamorphosed material included in less metamorphosed terrains (e.g., Guillot et al., 2007; Avigad et al., 2003; Jolivet et al., 2005), except for the Western Gneiss in Norway (Root et al., 2005) and the Dabie-Hong'an block (Hacker et al., 2000). (4) Exhumation rates for the continental material are higher than for metamorphosed oceanic crust and sediments (Agard et al., in press; Duchêne et al., 1997), at least during the first stages of exhumation. For slow convergence zones, these rates often largely exceed not only the denudation rates but also the rock uplift rates inferred from the convergence rates and common kinematical models of accretion and subduction. This definitely implies some additional mechanisms for this exhumation stage. For example, for the Dora Maira unit (Western Alps), exhumation rates reached 34 mm yr^{-1} (i.e., several times the convergence rate, Rubatto and Hermann, 2001) before later decreasing to 16 mm yr^{-1} and then to 5 mm yr^{-1}. A similar evolution of exhumation rates was found for Norway (~10–11 mm yr^{-1}, Carswell et al., 2003; Terry et al., 2000), Himalaya (30 to 80 mm yr^{-1}, Hermann et al., 2001; O'Brien et al., 2001; Parrish et al., 2006), Betic Cordillera

* Corresponding author. Laboratoire de Tectonique, Université Pierre et Marie Curie-Paris 6, CNRS, UCP, Case 129-4 place Jussieu 75252 Paris, France. Tel.: + 33 2 23 23 60 95; fax: +33 2 23 23 67 80.
E-mail address: philippe.yamato.rennes1@gmail.com (P. Yamato).

0012-821X/$ – see front matter © 2008 Elsevier B.V. All rights reserved.
doi:10.1016/j.epsl.2008.03.049

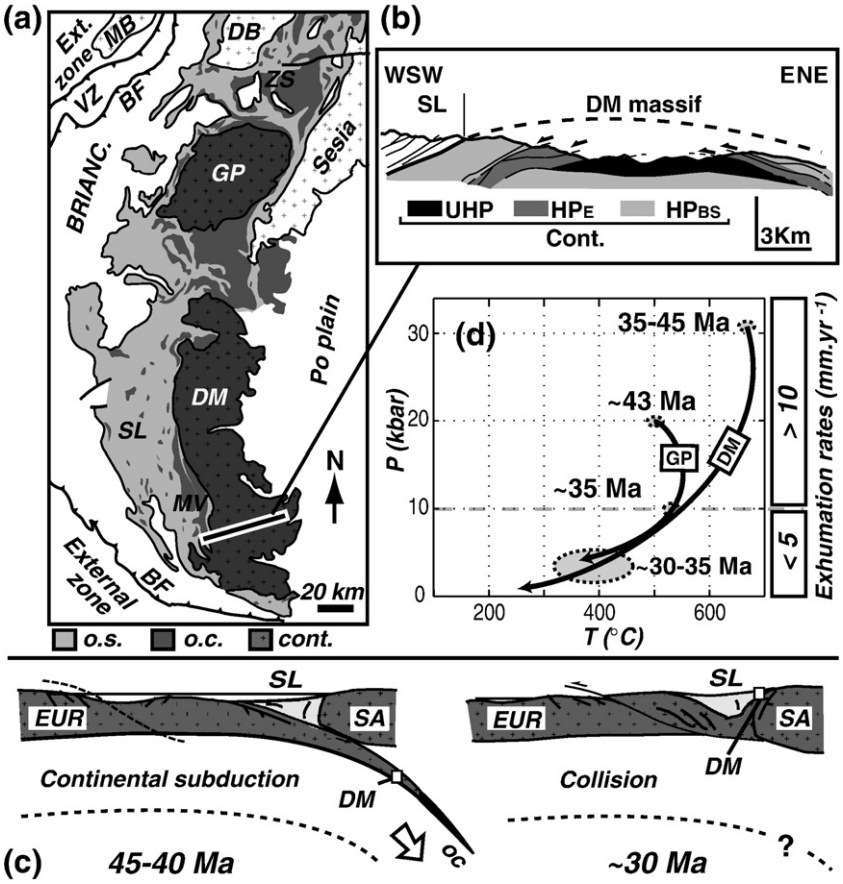

Fig. 1. Compiled data for the continental units from the western Alps. (a) Localisation of the continental (cont.), oceanic crust (o.c.) and sedimentary (sed.) units. (b) Schematic cross-section through the Dora Maira massif (after Henry et al., 1993) showing the lenses of UHP rocks within les metamorphosed units (HPE: high-pressure eclogites; HPBS: high-pressure blueschists). (c) Simplified evolution of the European passive margin continental subduction (Eocene) toward collision stage (Oligo–Miocene). Adapted from (Agard and Lemoine, 2005). (d) *P–T–t* path evolution for the continental units and exhumation rates estimates. Data are taken from (Duchêne et al., 1997; Le Bayon and Ballèvre, 2006; Henry et al., 1993). Abbreviations: Brianc., Briançonnais; DB, Dent Blanche; DM, Dora Maira; EUR, European margin; GP, Gran Paradiso; MB, Mont Blanc; MV, Monviso; SA, southern Alps; SL, Schistes Lustrés; VZ, Valais zone; ZS, Zermatt-Saas.

(22.5 mm yr^{-1}, De Jong, 2003) and Papua-New Guinea (>17 mm yr^{-1}, Baldwin et al., 2004). In all cases, the later rates decrease to values lower than 10 mm yr^{-1} (e.g., Terry et al., 2000; De Jong, 2003).

For these reasons, the first aim of this study is to build an unconstrained numerical thermomechanical (self-consistent) model explaining the most enigmatic first-order features of continental exhumation processes, with a particular focus on slow convergence zones. Indeed, these zones are expected to exhibit more complex behaviour and more deviations from the conceptual kinematic models of subduction since in the case of slow convergence, the system Peclet numbers (Pe, ratio of advection to diffusion time scale) may fall below 10 suggesting that continental subduction needed for burial of HP rocks is only marginally possible and may be associated with gravitational instabilities or should be highly short-lived (Toussaint et al., 2004).

The Western Alps were chosen because of the wealth of available data that can be used to constrain our models. The new experimental approach is needed to circumvent typical drawbacks of previous models of continental exhumation. For example, the analogue models (e.g., Chemenda et al., 1995) predict the exhumation of crustal-scale rock volumes, which is not generally observed in natural settings. These models are not thermally coupled and thus do not allow to account for important thermally controlled properties, such as slab strength and buoyancy, or for comparisons with *P–T* data. Numerical models reproducing some of the major characteristics of the Alpine belt structure were published by Pfiffner et al. (2000), but these models cannot be really used to test the mechanical viability of the models or for the comparison with *P–T* data because their results are preconditioned by a fixed internal "boundary" condition (subduction point, or "S-point") imposed inside the model area and maintained during the experiments. The models of Burov et al. (2001), Toussaint et al. (2004) and Burov and Yamato (2007) are free of such constraints but were not actually designed to compute synthetic thermodynamically consistent *P–T–t* (time) paths for continental domains, which makes it difficult to test their results against the petrologic data. Finally, Stöckhert and Gerya (2005) designed a thermodynamically coupled, yet still kinematically constrained, thermomechanical model and obtained *P–T–t* paths whose shapes are in a good agreement with the Alpine settings. However, in contrast with the available geological observations (Fig. 1), the exhumation of HP-UHP material implies only the overriding continental plate in their experiment.

We herein propose a new thermomechanical model that implies realistic visco-elasto-plastic rheologies, thermodynamically consistent progressive density changes, erosion-sedimentation processes and does not require any pre-imposed internal boundary conditions. The results of our best fitting experiments are then used to discuss the mechanisms of burial/exhumation.

2. Observational constraints on the continental subduction in the Western Alps

The large structural and petrological data sets available for the Western Alps were used to constrain our model. In the Western Alps, HP units also include oceanic material (e.g., Monviso, Zermatt-Saas). Exhumation of these mafic units was addressed in recent detailed

modeling study by Yamato et al. (2007), and therefore we focus here on continental material only. Fig. 1 summarizes the main points concerning the existing data for the internal crystalline (ICM) Dora Maira (UHP) and the Gran Paradiso (HP) massifs. These small metamorphic units of continental origin (e.g., Chopin, 2003; Le Bayon and Ballèvre, 2006) are located in the internal zones (to the east) of the Alpine belt structure (Fig. 1a and b).

Although the geodynamic context of the Alps is still discussed (e.g., Le Pichon et al., 1988; Marchant and Stampfli, 1997), the following points are widely accepted. According to the data, HP-UHP continental units of the Western Alps constitute the remnants of the European passive margin, which reached the subduction zone at ~45 Ma (e.g., Deville et al., 1992; Michard et al., 1996; Rosenbaum and Lister, 2005), after the subduction of the Liguro–Piemontese ocean (~100 to 40–45 Ma). Continental HP-UHP rocks were buried under the Schistes Lustrés complex before being exhumed to intermediate depths at ~35 Ma at the rear of the belt, when the collision began (Fig. 1c, Agard and Lemoine, 2005). Von Blanckenburg and Davies (1995) proposed that this exhumation, which coincided with a period of magmatic activity at around 40–35 Ma, was induced by a lithospheric slab break-off.

The current detailed knowledge of the Western Alpine geodynamics largely owes to the abundance of pressure-temperature-time data. A simplified compilation of these data for the main metamorphic units of the Western Alps can be found in Yamato et al. (2007). The *P–T–t* values for the main continental units are also summarized in Fig. 1d. The exhumation rates of these units, however, should be considered with caution because the age estimates of the UHP metamorphism are still debatable (Duchêne et al., 1997; Agard et al., 2002; Gebauer et al., 1997; Henry et al., 1993), although the majority of the recent ages fall in the interval between 35 and 45 Ma. Nevertheless, fast initial exhumation rates are additionally confirmed from observations in other continental convergent zones (e.g., Himalaya, Norway). Exhumation of continental material thus corresponds to a short event (<10 Myr) in the Alpine belt formation, with a first stage of exhumation at a very fast rate (>10 mm yr^{-1}) and the second stage at much lower rate (<4 mm yr^{-1}; see Agard et al., in press, 2002 for further details).

3. Numerical approach

We used the visco-elasto-plastic thermomechanical numerical code PARA(O)VOZ. This code incorporates the same mechanical solution kernel as the well-known F.L.A.C. (Fast Lagrangian Analysis of Continua) algorithm (Cundall, 1989) and particle-in-cell technique for particle tracing and interpolation of variables during dynamic remeshing. This code solves simultaneously the Newtonian motion equations and heat transfer equations in large-strain Lagrangian formulation:

$$\frac{\rho Dv_i}{Dt} - \frac{\partial \sigma_{ij}}{\partial x_j} - \rho g_i = 0, \tag{1}$$

$$\frac{D\sigma}{Dt} = F(\sigma, \mathbf{u}, \nabla \dot{\mathbf{u}}, \ldots T \ldots), \tag{2}$$

where **u** stands for displacement vector, ***v*** is velocity, ρ is density, t is time, g is acceleration due to gravity, D and overdot is material derivative and σ is the Lagrangian stress, T is temperature. F denotes functional relationship for visco-elasto-plastic constitutive law (we use Mohr–Coulomb criterion for plasticity and non-linear power law for viscous flow, Table 1, Ranally and Murphy, 1987; Goetze and Evans, 1979; Carter and Tsenn, 1987). The Eqs. (1)–(2) are coupled with the heat transfer Eq. (3). The Boussinesq approximation is used for thermal density variations in the experiments with no phase changes (Eq. (4), left expression), otherwise the density is updated as a function of P and T (Eq. (4), right expression) using the thermodynamic (free energy minimization) algorithm THERIAK (De Capitani, 1994). Finally, we account for surface processes using commonly inferred diffusion erosion/sedimentation (Eq. (5)):

$$k \cdot \mathrm{div}(\nabla T) - \rho C_p \frac{DT}{Dt} + H_r = \mathbf{v} \nabla T, \tag{3}$$

$$\rho = \rho_0 (1 - \alpha (T - T_0)) \quad \text{or} \quad \rho = f(P, T) \tag{4}$$

$$\frac{\partial^2 h}{\partial t^2} = k_{\mathrm{ero}} \mathrm{div}(\nabla h) \tag{5}$$

where v is the velocity vector, C_p is the specific heat, k is the thermal conductivity, H_r is the internal heat production per unit volume, α is the coefficient of thermal expansion, h is surface topography and k_{ero} is the coefficient of erosion (see Tables 1 and 2).

Apart from the abundant F.L.A.C. literature, this in-house geodynamic version of the algorithm was described in detail in (Burov et al., 2001; Yamato et al., 2007; Le Pourhiet et al., 2004). The particle-in-cell technique (9 particles, or markers, per cell) is used to minimize numerical diffusion due to remeshing (see Yamato et al., 2007 for details). In particular, the marker-based remeshing permits to model very slow-rate convergence processes (few mm yr^{-1}) typical of the

Table 1
Parameters used in our model

Physical parameters			
All rocks		$\rho = f(P,T)$ calculated using THERIAK (kg m^{-3}) Friction angle = 30°	
Upper continental crust		Material: quartz[a] Thermal conductivity: 2.5 W m^{-1} °C^{-1} Thermal diffusivity: 8.3 × 10^{-7} m^2 s^{-1} Lamé constants: $\lambda = \mu = 3 \times 10^{10}$ Pa Cohesion: 20 × 10^6 Pa	
Lower continental crust		Material: diabase[a] Thermal conductivity: 2.5 W m^{-1} °C^{-1} Thermal diffusivity: 6.7 × 10^{-7} m^2.s^{-1} Lamé constants: $\lambda = \mu = 3 \times 10^{10}$ Pa Cohesion: 20 × 10^6 Pa	
Sediments		Material: quartz Thermal conductivity: 2 W m^{-1} °C^{-1} Thermal diffusivity: 8.3 × 10^{-7} m^2 s^{-1} Lamé constants: $\lambda = \mu = 1 \times 10^{10}$ Pa Cohesion: 1 × 10^6 Pa	
Oceanic crust		Material: olivine Thermal conductivity: 3.5 W m^{-1} °C^{-1} Thermal diffusivity: 8.75 × 10^{-7} m^2 s^{-1} Lamé constants: $\lambda = \mu = 3 \times 10^{10}$ Pa Cohesion: 20 × 10^6 Pa	
Mantle		Material: olivine Thermal conductivity: 3.5 W m^{-1} °C^{-1} Thermal diffusivity: 8.75 × 10^{-7} m^2 s^{-1} Lamé constants: $\lambda = \mu = 4 \times 10^{10}$ Pa Cohesion: 300 × 10^6 Pa	
Material creep parameters[b]			
Quartz	$n = 3$	$A = 6.8 \times 10^{-6}$ MPa^{-n} s^{-1}	$E = 1.56 \times 0^5$ J mol^{-1}
Diabase	$n = 3.05$	$A = 6.3 \times 10^{-2}$ MPa^{-n} s^{-1}	$E = 2.76 \times 10^5$ J mol^{-1}
Olivine	$n = 3$	$A = 7.0 \times 10^3$ MPa^{-n} s^{-1}	$E = 5.10 \times 10^5$ J mol^{-1}
Thermal parameters[c]			
T_0; T_{hl}		0 C; 1330 °C	
h_l; h_c; h_r		100 km; 40 km; 10 km	
H_s		1.10^{-9} W kg^{-1}	
ρ_c; ρ_m		2800 kg m^{-3}; 3300 kg m^{-3}	
k_c; k_m		2.5 W m^{-1} K^{-1}; 3.5 W m^{-1} K^{-1}	
C_m		10^3 J kg^{-1} K^{-1}	
T(age)		115 Ma	

[a] In the reference experiment.
[b] Creep parameters for Quartz, Diabase and Olivine are respectively taken from (Ranally and Murphy, 1987; Goetze and Evans, 1979; Carter and Tsenn, 1987).
[c] Significance of each term is given in Appendix A.

Table 2
Parametric study

Name of the experiment	Convergence rate (mm yr^{-1})	k^{a}_{eros} (m^2.yr^{-1})	Material implied[b]				HP-UHP subducting continental crust exhumation?
			SPUC	SPLC	OPUC	OPLC	
Alps_Ref.	6	3000	Qtz	Diab	Qtz	Diab	Yes
Alps_03	3	–	–	–	–	–	Yes
Alps_09	9	–	–	–	–	–	Yes
Alps_12	12	–	–	–	–	–	Yes
Alps_30	30	–	–	–	–	–	No
Alps_ero500	–	500	–	–	–	–	No
Alps_ero1000	–	1000	–	–	–	–	No
Alps_ero1500	–	1500	–	–	–	–	No
Alps_ero2000	–	2000	–	–	–	–	No
Alps_ero4000	–	4000	–	–	–	–	Yes
Alps_ero5000	–	5000	–	–	–	–	Yes
Alps_ero6000	–	6000	–	–	–	–	Yes
Alps_QQ[c]	–	–	Qtz	Qtz	Qtz	Qtz	No
Alps_DD[c]	–	–	Diab	Diab	Diab	Diab	No
Alps_QD[c]	–	–	Qtz	Qtz	Diab	Diab	No
Alps_DQ[c]	–	–	Diab	Diab	Qtz	Qtz	No
Alps_QM[c]	–	–	Qtz	Qtz	Qtz	Diab	No
Alps_DM[c]	–	–	Diab	Diab	Qtz	Diab	No
Alps_MQ[c]	–	–	Qtz	Diab	Qtz	Qtz	No
Alps_MD[c]	–	–	Qtz	Diab	Diab	Diab	Yes

[a]Erosion coefficient. [b]Abbreviations: SPUC, subducting plate upper crust; SPLC, subducting plate lower crust; OPUC, overriding plate upper crust; OPLC, overriding plate lower crust; Qtz, quartz; Diab, diabase. [c]Reading key for the experiment testing rheology of the continental crust. After underscore symbol, the two letters correspond to the rheological property of respectively the subducting continental crust and the overriding continental crust. Q: quartz (single-layer crust), D: diabase (single-layer crust), M: mixed (double-layer crust composed by quartz and diabase respectively for the upper and the lower continental crust).

continental stage of Alpine collision. Passive markers are also needed to calculate synthetic *P–T–t* paths (Yamato et al., 2007).

4. Model setup

The model setup is based on the existing knowledge for the Western Alps (geometry, age of the lithosphere, convergence rates) and/or the results of earlier parametric study (erosion, rheology of the crust, convergence rates). Initial and boundaries conditions used in our experimental framework are described below and in Table 1.

4.1. Initial geometry

The initial dimensions of the model box are 399 km (height) by 1482 km (width) with spatial mesh resolution of 3×3 km (Fig. 2a). The initial geometry implies a continental plate that barely started to subduct and only reached the bottom of the oceanic accretionary wedge. This situation corresponds to that projected for the Western Alps at the beginning of the subduction of the thin continental margin (Dora Maira), at ~45–50 Ma (Fig. 1c). The dip of subduction is arbitrarily set to 30°, which is of minor importance, as the model is free to chose an optimal dip on further stages of evolution.

4.2. Thermal structure

The initial geotherm, presented in Fig. 2b, is based on plate cooling model modified from Parsons and Sclater (1977) assuming a multi-layer cooling half-space. This model, described in detail in Appendix A and Table 1, is unstationary and depends on the thermal age of the lithosphere (thermotectonic age) and on the radiogenic heat production of the crust. Considering thermal rejuvenation due to the spreading of the Tethyan Ocean at ~160 Ma (Lemoine et al., 1986), it is reasonable to suppose the initial thermotectonic age for the continental lithosphere of ~115 Ma (=160 Ma–45 Ma). This age is applied for both the subducting and the overriding plate.

4.3. Rheology and parameters

Commonly inferred parameters are used for establishing the lithosphere rheology (Ranally and Murphy, 1987; Goetze and Evans, 1979; Carter and Tsenn, 1987). The yield-strength envelope resulting from the assumed rheology (Table 1) and from the thermal profile chosen (Fig. 2c) is presented in Fig. 2d. The choice of these parameters was discussed in Yamato et al. (2007) and is therefore not recalled here. The rheological structure of the Alpine crust is still not well known. For this reason, an additional parametric study was carried out (see Section 5.3) in order to test the influence of a single- or a double-layer crustal rheology on the exhumation processes of the metamorphic rocks.

Quartz and diabase rheologies were used respectively for the upper and the lower continental crust in the experiments that tested double-layer crustal structure with two brittle-ductile transition zones (Fig. 2c). Quartz and diabase rheologies were also used for the entire crust (single layer crustal structure) for end-member cases of very weak and very strong (Fig. 2d) crust, respectively.

4.4. Boundary conditions

For lateral boundary conditions, we apply horizontal convergence at constant rate at both sides of the model (allowing free slip in the vertical direction). The upper surface is free and is affected by surface erosion and sedimentation. At the bottom of the model, we apply Winkler's pliable basement (i.e., hydrostatic equilibrium) with free horizontal slip condition. The Winkler's condition is such that the model overlies an infinite space filled with an inviscible fluid having a small density contrast (10 kg m^{-3}) with the lower part of the model.

5. Constraints from the parametric study

A preliminary parametric study was first carried out to test the model sensitivities to the implied convergence and erosion rates and rheological composition of the crust (Table 2). This study (see below) was necessary to justify our choice of the material parameters used in the reference experiment. For comparison, the general evolution of the reference experiment is presented on Fig. 3 and will be discussed later (Section 6.1).

5.1. Influence of the convergence rates

The entire range of relevant values of the convergence rate has been tested (see Table 2), from very slow (3 mm yr^{-1}) to moderate

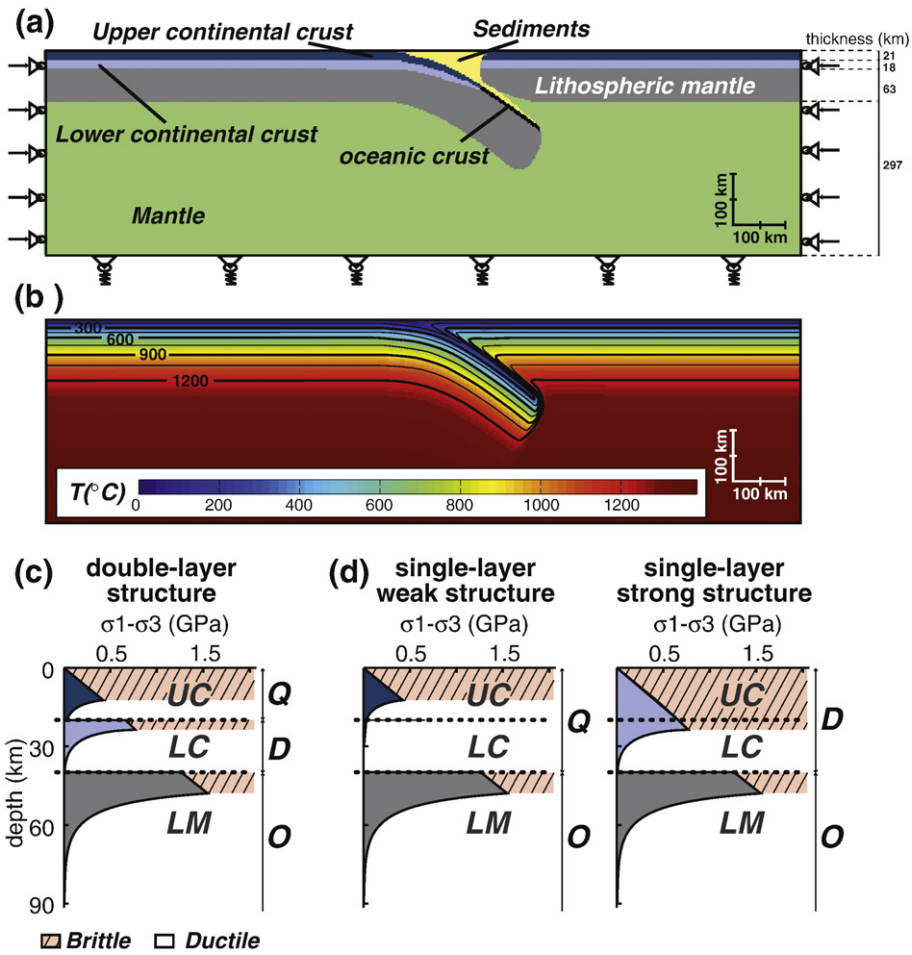

Fig. 2. Model setup. (a) Initial morphology and boundaries conditions. The horizontal arrows correspond to velocity boundary conditions imposed on the sides of the model. The basement is Winkler isostatic. The top is free (+ erosion/sedimentation). (b) Thermal structure used in the models (c) representative viscous-elastic-plastic yield strength profile for the continental lithosphere derived from the assumed rheological parameters (Table 1) for a double-layer structure of the continental crust and the initial thermal field assuming a constant strain rate of 10^{-14} s^{-1}. In the experiments, the strain rate is highly variable both vertically and laterally. (d) Same graphics for a single-layer structure using quartz (left) and diabase (right). Abbreviations: UC, upper crust; LC, lower crust; LM, lithospheric mantle.

(30 mm yr^{-1}). The obtained results show that exhumation of continental crustal material occurs in the experiments implying low convergence velocities (≤12 mm yr^{-1}). In contrast, for higher convergence rates (30 mm yr^{-1}), the continental material from the subducting plate was never exhumed to the surface (Fig. 4a). In these experiments, the imposed rapid collision does not allow for the creation of sufficient space between the upper and lower plates, inhibiting the possibility for deep material to come back to the surface (Fig. 4a). Moreover, in the cases where exhumation of continental crust occurs (convergence rates ≤12 mm yr^{-1}), the exhumation rate patterns are almost constant (with peak exhumation values of ~10 mm yr^{-1}; Fig. 4b), except for the experiment at 12 mm yr^{-1} that constitutes a threshold above which exhumation does not occur. The exhumation occurs in two stages, with the first-stage rates largely independent of the convergence rates. As suggested in Burov et al. (2001), these first-stage rates probably refer to Stokes velocity, that is conditioned by the viscosity and density contrast between the exhumed material (plus the matrix) and its environment.

5.2. Influence of the erosion rates

Fig. 5a shows selected examples of the experiments testing different erosion rates. These rates have been varied by changing the erosion coefficients (Table 2, Fig. 5b). After 20 Myr of convergence, the predicted surface topography is nearly the same for all the experiments. These results supports the existence of an efficient dynamic feedback between the erosion, isostasy and tectonic forcing that ensure stable morphology through time via re-adjustment of subsurface reaction to the changes in surface loading, and *vice versa* (Avouac and Burov, 1996; Burov and Toussaint, 2007). Moreover, the morphology at depths greater than ~50 km is largely independent of the surface erosion rate (Fig. 5a), a result which appears to be specific of slow convergence rate experiments (by comparison with the fast convergence rate experiments of (Avouac and Burov, 1996; Burov and Toussaint, 2007). In contrast, erosion strongly controls the latest stage of exhumation occurring near the surface. In particular, surface exhumation of continental crustal material is possible only for the values of erosion coefficient greater than 2000 m^2 yr^{-1} (Table 2, Fig. 5a). Thus, erosion rate plays a major role during the latest stages of exhumation but does not impact on the first deep stage, as also shown in other recent studies (e.g., Warren et al., 2008a). This result explains the two-stage evolution of the exhumation rate observed in the experiments: the first stage of rapid exhumation (>10 mm yr^{-1}) from great depth, which is mainly controlled by the buoyancy and viscous forces, and the slow second stage, which is controlled by the erosion rate yielding exhumation rates (<5 mm yr^{-1}) on the same order as the erosion rates (Fig. 5b).

5.3. Influence of the crustal rheology

We have carried out different experiments to test the influence of the crustal rheology on the burial/exhumation processes. Three types of rheological profile for the continental crust have been tested: (1) a

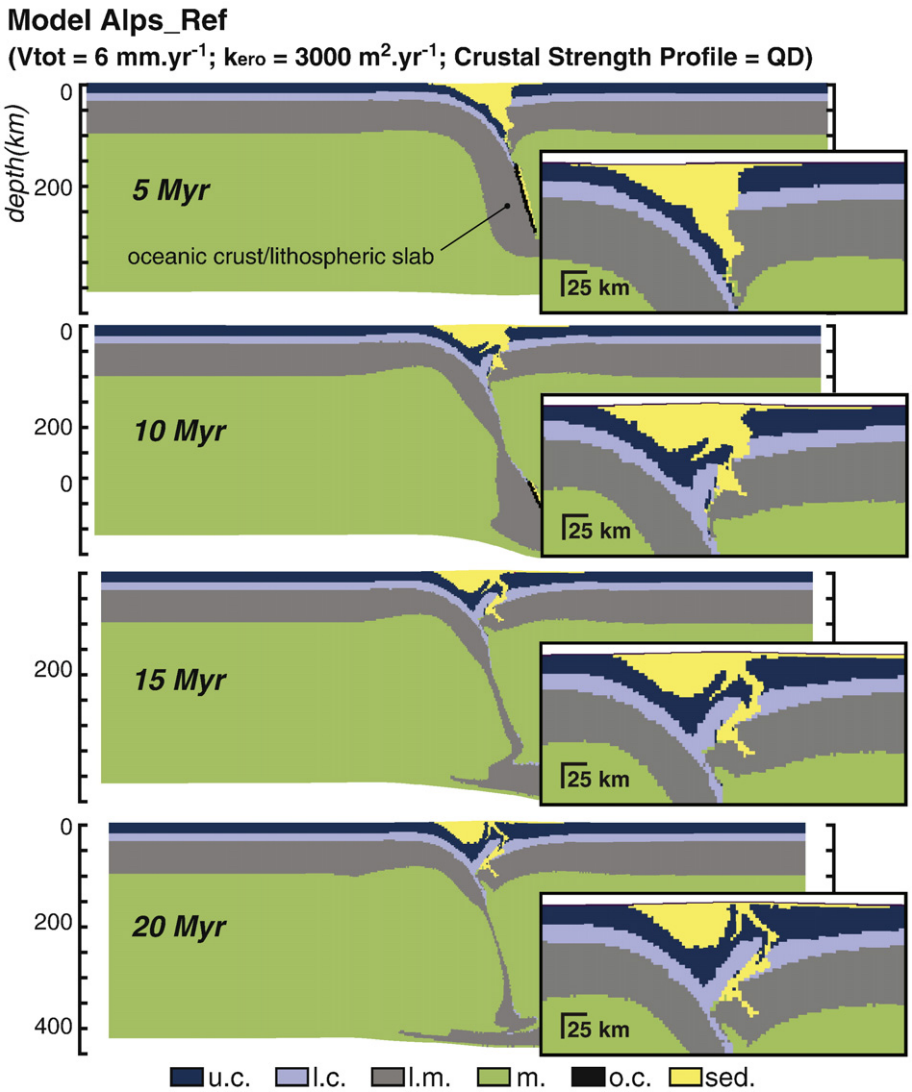

Fig. 3. Large scale evolution and zoom plots of the model during 20 Ma for the reference experiment. Abbreviations: u.c., upper crust; l.c., lower crust; l.m., lithospheric mantle; m., mantle; o.c., oceanic crust; sed., sediments; V_{tot}, convergence rate; k_{ero}, erosion coefficient; QD: Quartz-Diabase double layer structure (Fig. 2c).

double-layer structure (Fig. 2c) simulated by quartz and diabase for the upper and lower crust, respectively, (2) a weak single-layer structure (Fig. 2d) where quartz is used for the entire crust and (3) a strong single-layer structure where the entire crust has a diabase rheology (Fig. 2d). These experiments are described in Table 2 and representative predicted morphologies (after 20 Myr of experiment) are shown in Fig. 6. In the experiments with weak single-layer continental crust, the subduction does not persist, slab break-off occurs early, and neither burial nor exhumation is possible. In contrast, in the experiments implying strong single-layer continental crust, the continental crust is buried to very important depth (>100 km), yet, no exhumation occurs because the mechanical coupling between the upper and the lower continental crust is too strong. Both burial and exhumation of the continental material only took place in the models where a double-layer structure for the continental crust permitted the mechanical decoupling between the upper and the lower continental crust.

5.4. Summary and parameters choice for a reference experiment

This parametric study shows that exhumation of HP-UHP continental rocks from the subducting plate is most favoured for slow convergence rates (<1.5 cm yr^{-1}), high erosion/sedimentation rates (>2000 m^2 yr^{-1}) and occurs only in the cases implying a rheologically decoupled double-layer (quartz-diabase) continental crust. Under such conditions, the obtained results (predicted topography, structure, shapes of *P–T–t* paths, exhumation rates) are in a good agreement with the observational data for the Alps. The selected reference experiment described below thus implies convergence of two continental lithospheric plates with double-layer crustal structure (Fig. 2a and c). The total convergence rate is 6 mm yr^{-1} and the erosion/sedimentation coefficient is 3000 m^2 yr^{-1}.

6. Results

6.1. Large-scale evolution of the model

Fig. 3 shows the morphologies predicted by the reference model during the first 20 Myr of the reference experiment. During the first 5 Myr, the continental lithosphere is buried down to UHP depths and exhumation begins. At the same time, the subducted oceanic slab is progressively detached from the continental slab. 15 Myr are then needed for the deepest continental material (~100 km) to come back to the surface at the rear of the accretionary wedge. This exhumation is fast at the first stage: after ~10 Myr, the exhumed rocks already reach the bottom of the continental crust (~35–40 km), implying an exhumation

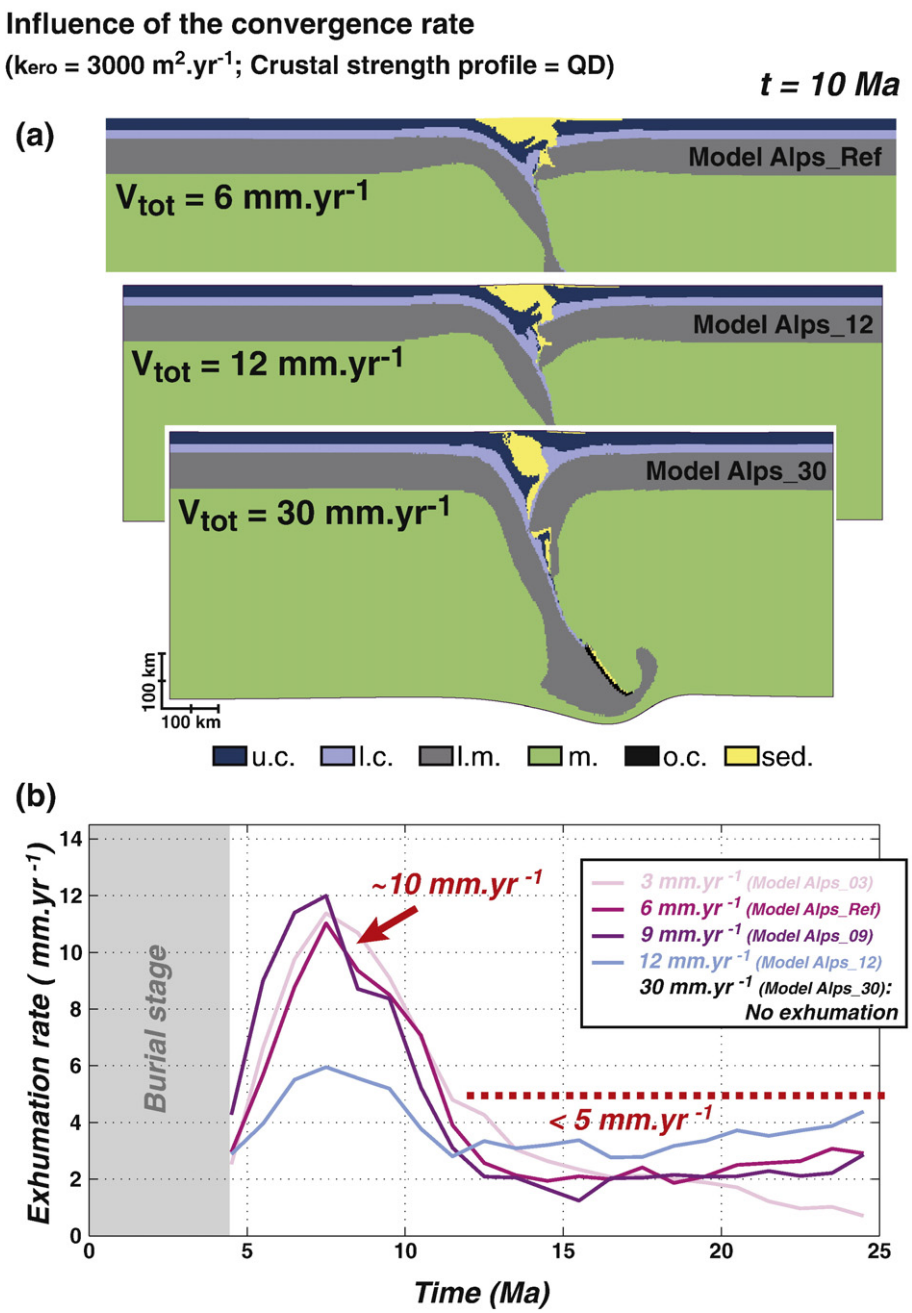

Fig. 4. Results from the parametric study (a) Morphologies of the models at 10 Myr for different convergence rates (other notations are as for Fig. 3). (b) Average of exhumation rates obtained in our models for all the markers in exhumation.

rate of >10 mm yr^{-1}. It is also noteworthy that UHP exhumation occurs while the oceanic lithosphere is still attached to the subducting lithospheric plate, explaining the close association between oceanic eclogites and UHP rocks in the Western Alps (Agard et al., in press, 2002). Although only ~5 Myr are needed for the UHP rocks to travel vertically over 60–65 km, 10 Myr more are needed before they reach the surface during the second stage where the exhumation rates drop to ~4 mm yr^{-1}. The predicted topographic evolution, which represents one of the important validation criteria for our model, appears to be highly realistic during the entire experiment, with maximal topographic relief smaller than 4 km (Fig. 5b).

6.2. Predicted P–T–t paths

Fig. 7a shows the location of markers at the beginning and at the end of the numerical experiment. The *P–T–t* paths computed for all markers located in the continental crust are presented on Fig. 7b. A more detailed analysis of some of them is shown on Fig. 7c. The shape of the calculated *P–T* paths, as well as the maximum *P* values reached and the *P–T* gradients are very close to natural data. Burial/exhumation of the continental crust occurs during the first ~10 Myr, during the convergence process, with exhumation rates similar to those recorded in the Western Alps (Fig. 7c). The experiment also shows that when collision begins, erosion or near-surface tectonic processes can only exhume rocks from crustal depths but not from deeper levels.

We note, however, that although the predicted *P–T* trends are compatible with the data, the predicted temperatures are colder (100–150 °C) than those inferred from the observed *P–T* paths, as in the experiments of Stöckhert and Gerya (2005) or Warren et al. (2008a,b). This discrepancy may be due to the fact that, in our models, frictional heat production was set to zero (contrary to Burg and Gerya, 2005),

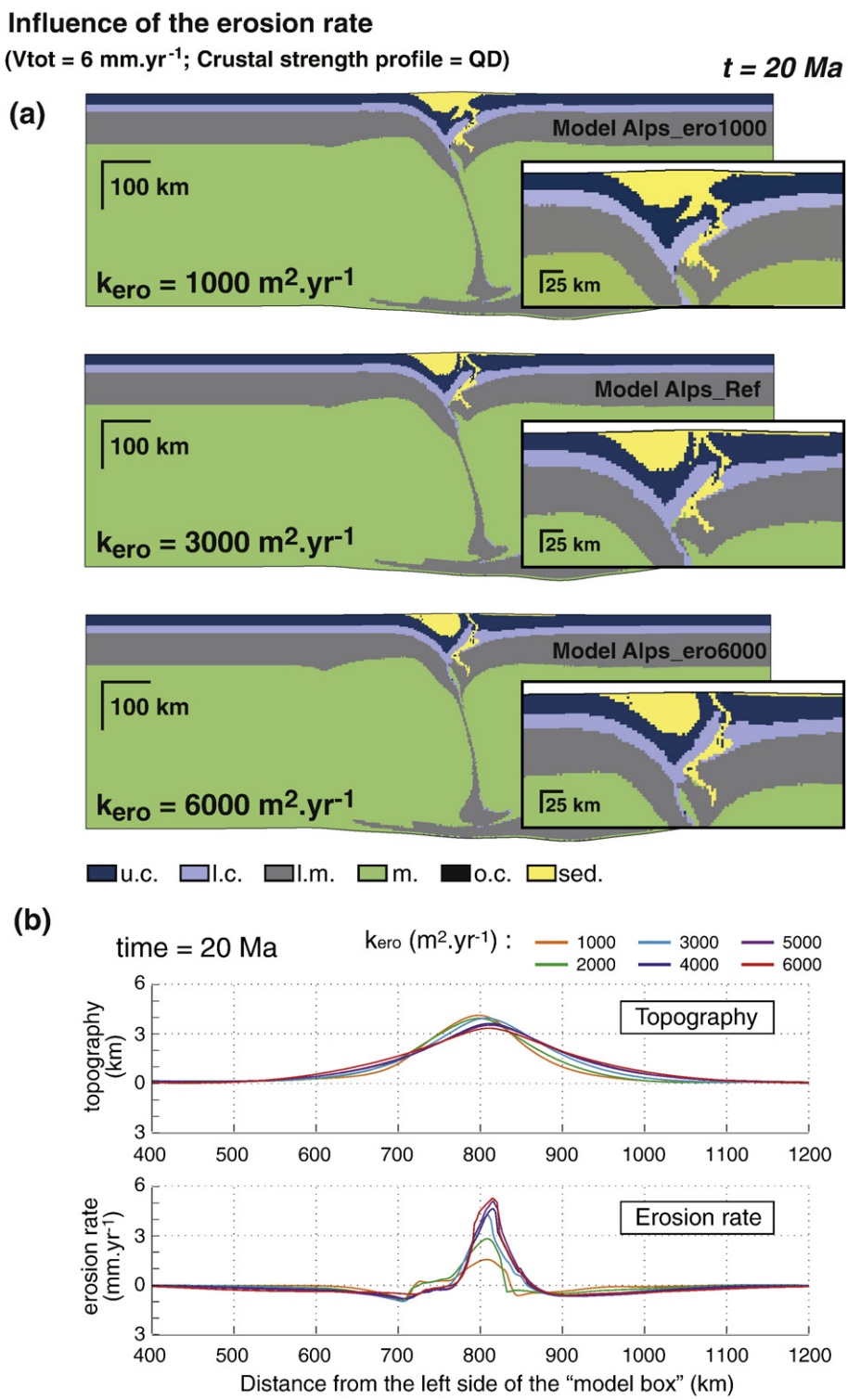

Fig. 5. (a) Morphologies of the models after 20 Myr of experiment for different erosion coefficients. Legend is as for Fig. 3. (b) Topography and erosion at 20 Myr obtained in different experiments testing the influence of the erosion coefficients.

and latent heat and partial melting are also neglected. The reason of doing so was to see how well the data can be fitted without additional heat sources or sinks, which allows one to isolate the amount of heat needed in addition to the heat diffusion-advection mechanisms. Accounting for heat production would increase the temperatures by ~100 °C (Turcotte and Schubert, 2002), bridging the gap with the data, as it was already done with success in some recent subduction models (Gerya et al., 2007; Faccenda et al., 2007). However, the actual parameters of the related mechanisms are difficult to constrain from any observational data available (see below): even if shear heating can be realistically accounted from conservation laws in a global sense, in case of delocalized deformation (convection models) there is much more uncertainty when one needs to treat localised temperature anomalies on shear bands, specifically in large-scale models. This uncetainty stems from scale-dependence of the predicted temperature variations associated with a number of reasons: (1) the local efficiency factor of conversion of the mechanical to thermal energy is unknown, and may be anything from 0.01 to 1; (2) the predicted

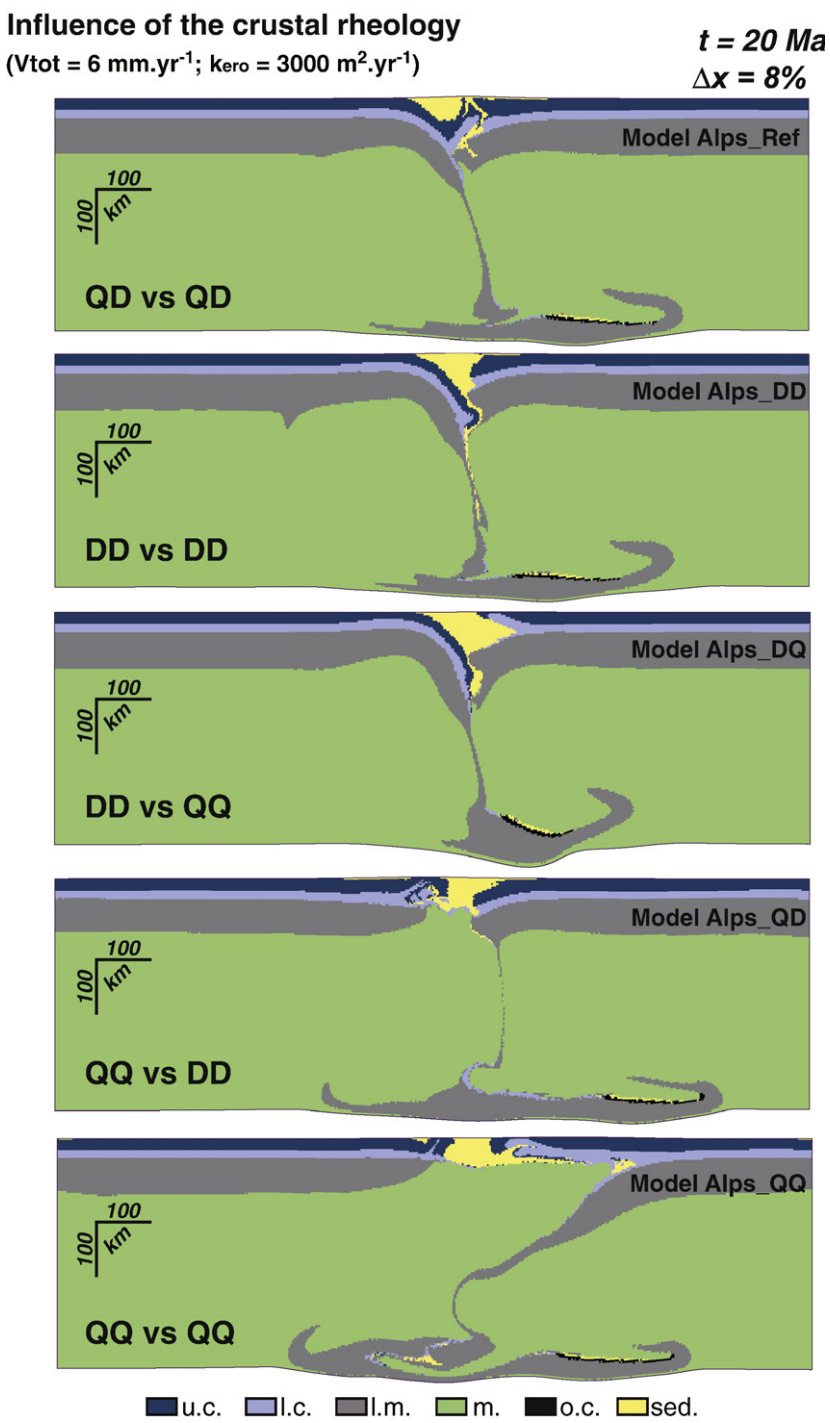

Fig. 6. Morphologies for the models at 20 Myr for different crustal strength profiles. Legend is as for Fig. 3. QD: quartz–diabase double-layer structure (Fig. 2c). QQ: weak single-layer structure simulated by quartz (Fig. 2d); DD: strong single-layer structure simulated by diabase (Fig. 2d). (Reading key: X vs Y means that rheological structure X is used for the subducting plate and Y rheological structure is used for the overriding plate).

temperature variations depend on local stress and strain rate and thus on the thickness of shear bands conditioned by numerical grid resolution; (3) the localized temperature highs are sensitive to the peculiarities of the assumed rheology laws, presence of fluids, thermal properties, variations in the subduction rate, etc.

6.3. Importance of crustal decoupling for exhumation mechanisms

We used passive markers to trace the *P–T–t* paths and trajectories of selected "rocks" in the model. The predicted thermal distributions combined with the predicted strain rate patterns (Fig. 8) also allow us to track the environment (ductile or brittle) in which each marker evolves. The experiments show that between 0 and 5 Myr (Fig. 8a), all of the subducting plate is buried, in particular, the marker "CC1" (Dora Maira equivalent, Fig. 7) reached a near 100 km depth. The marker "CC2" ("Gran Paradiso") was buried to nearly 50 km depth. The background deformation at these depths is ductile and intense (high strain rates ~10^{-14} s^{-1}).

Between 5 and 10 Myr (Fig. 8b), the direction of exhumation is at 90° from the slab dip. Exhumation proceeds from the zone of rheological decoupling between the lower crust and the lithosphere (hereafter noted LCDP — lower crustal decoupling point). The CC2

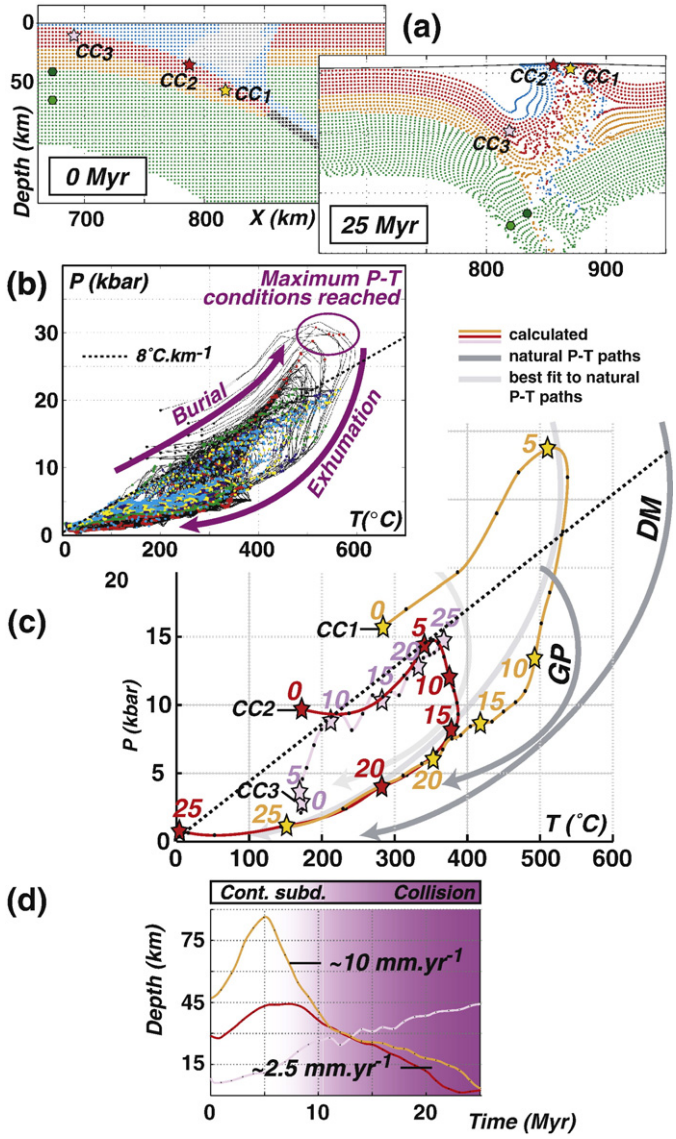

Fig. 7. (a) Location of passive markers at the beginning and at the end of the numerical experiments, showing also the position of points of specific importance discussed in the text. Markers of blue and grey colour correspond to initial sediments (Grey markers are those totally eroded after the 20 Myr of experiment. Red and orange markers correspond respectively to the upper crust and the lower crust. Green markers represent lithospheric mantle and black ones the oceanic crust. Abbreviations: CC, continental crust; SL, accretionary wedge sediments of the "Schistes Lustrés". (b) *P–T* evolution of all the pointers localized within the upper continental crust. (c) Example of *P–T–t* paths for pointers coming from the upper continental crust and comparison with the natural *P–T* path of the Western Alps. Color and symbols as for (a). GP: Gran Paradiso; DM: Dora Maira. (d) Evolution of pressure (and depth) for the selected markers through time. Switching heat dissipation "on" in the model would shift the predicted paths 100–150 °C along the *T* axis providing a perfect match with the petrology-based path.

marker follows a parallel exhumation trajectory, and the origin of this exhumation refers to the upper crustal decoupling point (UCDP), or zone of rheological decoupling between the upper and lower crust. The rheological decoupling zones at ~20 km depth for the upper crust (temperatures close to 350–400 °C) and at ~40 km depth for the lower crust (temperatures close to 600 °C), respectively, thus constitute privileged zones of intra-crustal decoupling controlling the exhumation of the UHP rocks. The fast first-stage exhumation occurs when the oceanic crust/lithosphere slab is not yet detached from the subducting plate (Figs. 3 and 8b). This indicates that slab break-off is not necessary to produce fast exhumation. These results and mechanisms are also in good agreement with the conclusions of some recent studies (e.g., Warren et al., 2008a,b). We note also that no surface exhumation occurs in the experiments implying only a single-layer crust (see Table 2, Fig. 6). In this case, subsurface exhumation actually takes place at the rear of the sedimentary wedge, but the exhumed material returns toward the overriding plate and never reaches the surface.

Between 10 and 15 Myr, a pure shear collision mechanism starts to dominate over the subduction mechanism of shortening. The exhumation of CC1 and CC2 still occurs in the same direction and originates from the LCDP and UCDP zones, but is much slower.

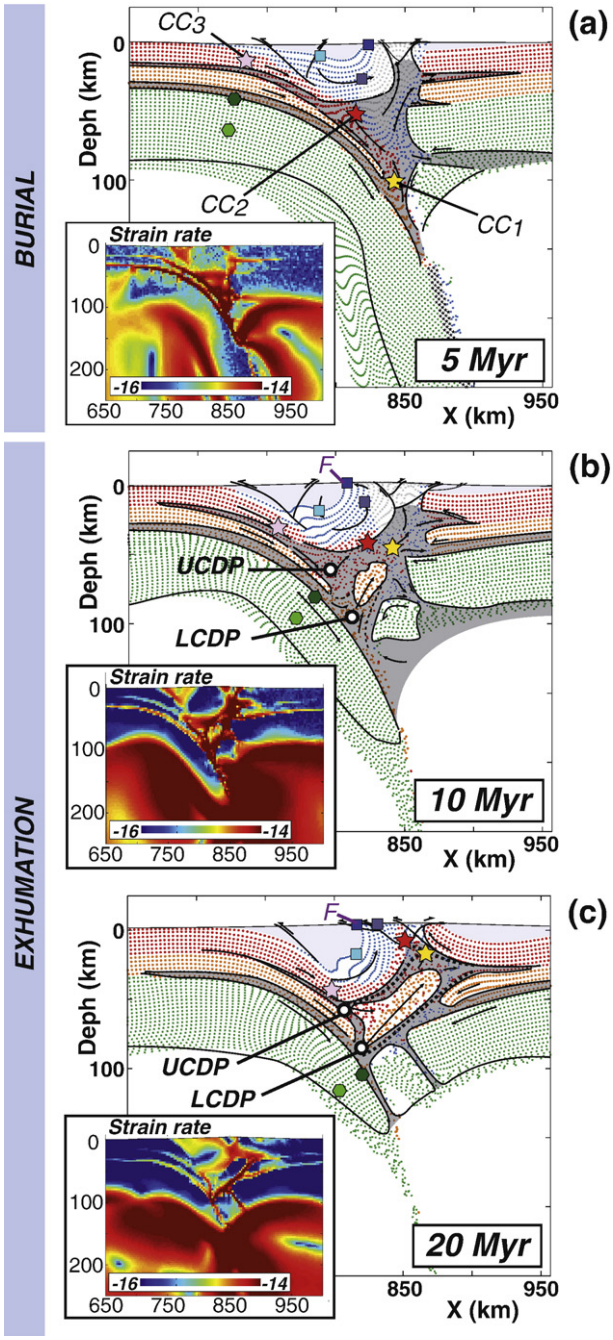

Fig. 8. Migration of markers and strain rate variations through time (see Fig. 7 for notations). Grey region corresponds to ductile domain between the subducting plate and the overriding plate. The position of the "*F* point" in the sedimentary accretionary wedge is virtually stable as well as that of two other characteristic points (UCDP and LCDP) (see text). Moreover, we note that within the pre-existing subjacent sedimentary accretionary wedge, sediments form a "rigid block", which stays non-deformed and moves, by rotation, around the stable point *F*. This mechanism would explain why "Schistes Lustrés" found at this place in the Western Alps are dated from the oceanic subduction.

Decoupling between the crust and the lithospheric mantle of the overriding plate now develops considerably, whereas the zone of point "CC3" continues to be buried. After 15 Myr (Fig. 8c), the exhumation of the areas of markers CC1 and CC2, which reach the brittle part of the crustal-scale accretionary wedge, is now very slow (~2.5 mm yr^{-1}, Fig. 7d), whereas the marker zone CC3 is still being buried (~40 km). This stage marks, in addition, a change of the vergence of the major faults at surface that now become synthetic with respect to the subduction plane. They are rooted in the great shear zone localized in the ductile part between the upper and the lower crust of the overriding plate.

7. Discussion and conclusion

Our model satisfactorily reproduces the overall geodynamics of the Western Alps (i.e., morphology (Fig. 3), topography (Fig. 5b), pressure peak (Fig. 7b), P/T gradient (dP/dT, Fig. 7c), exhumation rates (Fig. 7d), timing of the processes (Fig. 7c and d)), and provides important constraints on the mechanisms controlling exhumation in a slow continental subduction context:

(1) The exhumation of the continental material from the subducting plate (Chopin, 2003) occurs at the rear of the accretionary wedge, between the subducting and overriding plates, in agreement with the field observations for the Western Alps.
(2) Mechanical decoupling of two main ductile layers within the continental crust has a major role for deep exhumation. These critical layers mark the mechanical transition between the lithospheric mantle and the lower continental crust and the transition between the lower and the upper continental crust (LCDP and UCDP, respectively). They constitute the levels from which exhumation of the continental crust is initiated. The lower crust is not exhumed and is "underplated" below the upper continental crust of the overriding plate. Besides, one should note that only relatively small lenses of the continental material are exhumed, being inserted between less metamorphosed terrains.
(3) Lithospheric slab break-off occurs after the first stages of the exhumation. It is not needed for exhumation and does not impact on the exhumation rates.
(4) Continental subduction and the first fast stages of exhumation occur during the convergence as observed in many areas (e.g., Alps, Himalaya, Norway) and do not last more than ~10 Myr.
(5) In case of slow convergence rates (≤12 mm yr^{-1}), exhumation occurs in two stages at rates that are basically independent, at least at the first stage, of the convergence rate. The first "Stokes" stage results from the density contrast between the subducted crust and the surrounding mantle. Exhumation rates are fast (~10 mm yr^{-1}). The second stage originates from depths of 40–50 km, where the exhumed crustal material becomes more and more resistant (due to colder environment) and where the density contrast between the subducted and the surrounding rocks is reduced. Tectonic and surface processes control this second stage.
(6) Transition between the continental subduction and collision (i.e., when shortening is accommodated not only by subduction (simple shear) but also by pure shear thickening due to the accumulation of the exhumed/underplated continental material) corresponds to the moment when fast exhumation from great depth becomes impossible (Fig. 7d). During collision, only the second, slower exhumation stage persists.
(7) Although the discrepancies between the absolute values of temperature and those inferred from petrology data are on the order of 100–150 °C, the predicted trends dP/dT and P–T variations are very close to the data. This allows us to conclude that the main mechanisms of exhumation and burial are indeed reproduced in the model. The "missing" 100–150 °C, as in Stöckhert and Gerya experiments (Stöckhert and Gerya, 2005), most probably come from the absence of frictional heat sources in the model (Burg and Gerya, 2005). It is of trivial matter to estimate the amount of mechanical energy transferable to heat (Turcotte and Schubert, 2002), but the resulting temperature variations are much more uncertain because they depend on the effective thickness of shear bands in nature and in the model, as well as on many other unknown parameters that include material softening, fluid content, additional heating/cooling associated with concentration of radiogenic heat sources and thermal blanketing in the accretion prism, latent heat and partial melting, hydration-dehydration and so on. The real contribution of these sources at depth is unknown and one can be only confident in that ±100–150 °C maximal discrepancy with the data can be easily compensated in many ways (Gerya et al., 2007; Faccenda et al., 2007).
(8) In case of slow convergence and weak lower plate, surface processes have no significant impact on the deep (below 40 km depth) evolution of the collision zone. This is quite different from their role in the case of fast convergence zones involving strong subducting plates, where the erosion/sedimentation rate has a direct incidence on the amount of subduction and the geometry of the subduction channel (Burov and Toussaint, 2007).

Acknowledgements

Constructive reviews by C.J. Warren and T.V. Gerya are greatly appreciated. We also thank B. Goffé for fruitful discussions and G.W. Ernst for helping us to improve the earlier draft of the manuscript.

Appendix A. Initial thermal structure computation

To compute the initial continental geotherm T_{cont}, we use the Eq. (A1) taking into account, in T_{std}, the stationary part of the geotherm and contribution due to the radiogenic heat production H_s in the crust, and correction T(age) due to transient cooling of the lithosphere that depends on its age.

$$T_{cont}(z, \text{age}, H_s) = T_{std}(z, H_s) + T(\text{age}) \tag{A1}$$

Radiogenic contribution T_r in the crust depends of the thickness of the crust h_c, density ρ_c, radiogenic production H_s, radiogenic production decay depth h_r, and thermal conductivity coefficient k_c (Eq. (A2)):

$$T_r = \frac{\rho_c \cdot H_s \cdot h_r^2}{k_c} \cdot \left(1 - \exp^{-\frac{h_c}{h_r}}\right) \tag{A2}$$

Temperature T_m at Moho depth, h_c, is used for the calculation of the temperature for depths below the Moho and is given by:

$$T_m = T_0 + \frac{q_m}{k_c} \cdot h_c + T_r \tag{A3}$$

where T_0 and q_m correspond, respectively, to the temperature at the surface and the heat flux calculated at the Moho. This heat flux is given by:

$$q_m = \frac{T_{hl} - T_0 - T_r}{\frac{h_c}{k_c} + \frac{h_l - h_c}{k_m}} \tag{A4}$$

where T_{hl} is temperature at the thermal base of lithosphere (of a thickness h_l) and k_m is coefficient of thermal conductivity for the mantle.

Temperature at a depth z can thus be calculated as:

$$-\text{If } z \leq h_c: T_{std}(z) = T_0 + \frac{q_m}{k_c} \cdot z + T_r \tag{A5}$$

$$-\text{If } z \succ h_c: T_{std}(z) = T_m + q_m \cdot \frac{(z - h_c)}{k_m} \tag{A6}$$

This obtained temperature is then corrected for transient cooling that depends on thermotectonic age $T(\text{age})$ of the lithosphere using formulation from Parsons and Sclater (1977) adapted for the continental lithosphere.

$$T(\text{age}) = \frac{2}{\pi} \cdot \left(T_{h_l} - T_0\right) \cdot TT(\text{age}) \tag{A7}$$

where

$$TT(\text{age}) = \sum_{n=1}^{\infty} \frac{(-1)^{n+1}}{n} \cdot \exp\left(\frac{-k_m \cdot \pi^2 \cdot \text{age} \cdot n^2}{\rho_m \cdot C_m \cdot h_l^2}\right) \cdot \sin\left(\frac{n \cdot \pi \cdot z}{h_l}\right) \tag{A8}$$

with C_m and ρ_m are respectively the specific heat capacity and the density for the mantle. Values for the parameters used in our models for the initial geotherm are given in Table 1.

References

Agard, P., Lemoine, M., 2005. Faces of the Alps, Structure and Geodynamic Evolution, Comm. for the Geol. Map of the World, Paris. 48 pp.

Agard, P., Monié, P., Jolivet, L., Goffé, B., 2002. Exhumation of the Schistes Lustrés complex: in situ laser probe $^{40}Ar/^{39}Ar$ constraints and implications for the Western Alps. J. Metamorph. Geol. 20, 599–618.

Agard, P., Yamato, P., Jolivet, L., Burov, E., in press. Exhumation of oceanic blueschists and eclogites in subduction zones: timing and mechanisms, Earth Science Reviews.

Avigad, D., Chopin, C., Le Bayon, R., 2003. Thrusting and extension in the southern Dora-Maira ultra-high-pressure massif (Western Alps): view from below the coesite-bearing unit. J. Geol. 111, 57–70.

Avouac, J.P., Burov, E.B., 1996. Erosion as a driving mechanism of intracontinental mountain growth. J. Geophys. Res. 101 (8), 17747–17769.

Baldwin, S.L., Monteleone, B.D., Webb, L.E., Fitzgerald, P.G., Grove, M., Hill, E.J., 2004. Pliocene eclogite exhumation at plate tectonic rates in eastern Papua New Guinea. Nature 431, 263–267.

Burg, J.P., Gerya, T.V., 2005. The role of viscous heating in Barrovian metamorphism of collisional orogens: thermomechanical models and application to the Lepontine Dome in the Central Alps. J. Metamorph. Geol. 23, 75–95.

Burov, E., Toussaint, G., 2007. Surface processes and tectonics: forcing of continental subduction and deep processes. Glob. Planet. Change 58, 141–164.

Burov, E., Yamato, P., 2007. Continental plate collision, *P–T–t–z* conditions and unstable vs. stable plate dynamics: insights from thermo-mechanical modelling. Lithos. doi:10.1016/j.lithos.2007.09.014.

Burov, E., Jolivet, L., Le Pourhiet, L., Poliakov, A., 2001. A thermomechanical model of exhumation of high pressure (HP) and ultra-high pressure (UHP) metamorphic rocks in Alpine-type collision belts. Tectonophysics 342, 113–136.

Carswell, D.A., Brueckner, H.K., Cuthbert, S.J., Mehta, K., O'Brien, P.J., 2003. The timing of stabilisation and the exhumation rate for ultra-high pressure rocks in the Western Gneiss Region of Norway. J. Metamorph. Geol. 21, 601–612.

Carter, N.L., Tsenn, M.C., 1987. Flow properties of continental lithosphere. Tectonophysics 136, 27–63.

Chemenda, A.I., Mattauer, M., Malavieille, J., Bokun, A.N., 1995. A mechanism for syn-collisional rock exhumation and associated normal faulting: results from physical modelling. Earth Planet. Sci. Lett. 132, 225–232.

Chopin, C., 1984. Coesite and pure pyrope in high-grade blueschists of the Western Alps: a first record and some consequences. Contrib. Mineral. Petrol. 86, 107–118.

Chopin, C., 2003. Ultrahigh-pressure metamorphism: tracing continental crust into the mantle. Earth Planet. Sci. Lett. 212, 1–14.

Cundall, P.A., 1989. Numerical experiments on localization in frictional materials. Ingenieur-Archiv. 59, 148–159.

De Capitani, C., 1994. Gleichgewichts-Phasendiagramme: Theorie und Software, Beihefte zum European Journal of Mineralogy-Jahrestagung der Deutschen Mineralogischen Gesellschaft. 48 pp.

De Jong, K., 2003. Very fast exhumation of high-pressure metamorphic rocks with excess ^{40}Ar and inherited ^{87}Sr, Betic Cordilleras, southern Spain. Lithos 70, 91–110.

Deville, M., Fudral, S., Lagabrielle, Y., Marthaler, M., Sartori, M., 1992. From oceanic closure to continental collision: a synthesis of the 'Schistes Lustrés' metamorphic complex of the Western Alps. Geol. Soc. Amer. Bull. 104, 127–139.

Duchêne, S., Lardeaux, J.M., Albarède, F., 1997. Exhumation of eclogites: insights from depth-time path analysis. Tectonophysics 280, 125–140.

Faccenda, M., Gerya, T.V., Chakraborty, S., 2007. Styles of post-subduction collisional orogeny: influence of convergence velocity, crustal rheology and radiogenic heat production. Lithos. doi:10.1016/j.lithos.2007.09.009.

Gebauer, D., Schertl, H.P., Brix, M., Schreyer, W., 1997. 35 Ma old ultrahigh-pressure metamorphism and evidence for very rapid exhumation in the Dora Maira Massif, Western Alps. Lithos 41, 5–24.

Gerya, T.V., Perchuck, L.L., Burg, J.P., 2007. Transient hot channels: perpetrating and regurgitating ultrahigh-pressure, high-temperature crust-mantle associations in collision belts. Lithos. doi:10.1016/j.lithos.2007.09.017.

Goetze, C., Evans, B., 1979. Stress and temperature in the bending lithosphere as constrained by experimental rock mechanics. Geophys. J. R. Astron. Soc. 59, 463–478.

Green, H.W.I., 2005. Psychology of a changing paradigm: 40+ years of high-pressure metamorphism. International Geology Review 47, 439–456.

Guillot, S., Replumaz, A., Hattori, K.H., Strzerzynski, P., 2007. Initial geometry of Western Himalaya and ultra-high pressure metamorphic evolution. Journal of Asian Earth Sciences 30, 557–564.

Hacker, B.R., 2007. Ascent of the ultrahigh-pressure Western Gneiss Region, Norway. In: Cloos, M., Carlson, W.D., Gilbert, M.C., Liou, J.G., Sorensen, S.S. (Eds.), Convergent Margin Terranes and Associated Regions: A Tribute to W.G. Ernst. Geological Society of America Special Paper, vol. 419, pp. 171–184.

Hacker, B.R., Ratschbacher, L., Webb, L., McWilliams, M.O., 2000. Exhumation of ultrahigh-pressure continental crust in east central China: Late Triassic-Early Jurassic tectonic unroofing. J. Geophys. Res. 105, 13339–13364.

Henry, C., Michard, A., Chopin, C., 1993. Geometry and structural evolution of ultra-high pressure and high pressure rocks from the Dora Maira massif, Western Alps. J. Struct. Geol. 15, 965–981.

Hermann, J., Rubatto, D., Korsakov, A., Shatsky, V.S., 2001. Multiple zircon growth during fast exhumation of diamondiferous, deeply subducted continental crust (Kokchetav Massif, Kazakhstan). Contrib. Mineral. Petrol. 141, 66–82.

Jolivet, L., Raimbourg, H., Labrousse, L., Avigad, D., Leroy, Y., Austrheim, H., Andersen, T.B., 2005. Softening trigerred by eclogitization, the first step toward exhumation during continental subduction. Earth and Planetary Science Letters 237, 532–547.

Lallemand, S., Huchon, P., Jolivet, L., Prouteau, G., 2005. Convergence lithosphérique. 192 pp.

Le Bayon, B., Ballèvre, M., 2006. Deformation history of a subducted continental crust (Gran Paradiso, Western Alps): continuing crustal shortening during exhumation. J. Struct. Geol. 28, 793–815.

Lemoine, M., Bas, T., Arnaud-Vanneau, A., Arnaud, H., Dumont, T., Gidon, M., Bourbon, M., De Graciansky, P.C., Rudkiewicz, J.L., Megard-Galli, J., Tricart, P., 1986. The continental margin of the Mesozoic Tethys in the Western Alps. Mar. Pet. Geol. 3, 179–199.

Le Pichon, X., Bergerat, F., Roulet, M.J., 1988. Plate kinematics and tectonics leading to the Alpine belt formation: a new analysis. Geol. Soc. Amer. Special Papers 218, 111–131.

Le Pourhiet, L., Burov, E., Moretti, I., 2004. Rifting through a stack of inhomogeneous thrusts (the dipping pie concept). Tectonics 23, 1–14.

Liou, J.G., Tsujimori, T., Zhang, R.Y., Katayama, I., Maruyama, S., 2004. Global UHP metamorphism and continental subduction/collision: the Himalaya model. Int. Geol. Rev. 46, 1–27.

Marchant, R.H., Stampfli, G.M., 1997. Subduction of continental crust in the Western Alps. Tectonophysics 269, 217–235.

Michard, A., Goffé, B., Chopin, C., Henry, C., 1996. Did the Western Alps develop through an Oman-type stage? The geotectonic setting of high pressure metamorphism in two contrasting Thethyan transects. Eclogae geol. Helv. 89, 43–80.

O'Brien, P.J., Zotov, N., Law, R., Khan, M.A., Jan, M.Q., 2001. Coesite in Himalayan eclogite and implications for models of India–Asia collision. Geology 29, 435–438.

Parrish, R.R., Simon, J.G., Searle, M.P., Waters, D.J., 2006. Plate velocity exhumation of ultrahigh-pressure eclogites in the Pakistan Himalaya. Geology 34, 989–992.

Parsons, B., Sclater, T.G., 1977. An analysis of the variation of ocean floor bathymetry and heat flow with age. J. Geophys. Res. 82, 803–827.

Pfiffner, O.A., Ellis, S., Beaumont, C., 2000. Collision tectonics in the Swiss Alps: insight from geodynamic modeling. Tectonics 19, 1065–1094.

Ranally, G., Murphy, D.C., 1987. Rheological stratification of the lithosphere. Tectonophysics 132, 281–295.

Root, D.B., Hacker, B.R., Gans, P.B., Ducea, M.N., Eide, E.A., Mosenfelder, J.L., 2005. Discrete ultrahigh-pressure domains in the Western Gneiss Region, Norway: implications for formation and exhumation. J. Metamorph. Geol. 23, 45–61.

Rosenbaum, G., Lister, G.S., 2005. The Western Alps from the Jurassic to Oligocene: spatio-temporal constraints and evolutionary reconstructions. Earth-Sci. Rev. 69, 281–306.

Rubatto, D., Hermann, J., 2001. Exhumation as fast as subduction? Geology 29, 3–6.

Stöckhert, B., Gerya, T.V., 2005. Pre-collisional high pressure metamorphism and nappe tectonics at active continental margins: a numerical simulation. Terra Nova 17, 102–110.

Terry, M.P., Robinson, P., Hamilton, M.A., Jercinovic, M.J., 2000. Monazite geochronology of UHP and HP metamorphism, deformation, and exhumation, Nordøyane, Western Gneiss Region, Norway. Am. Mineral. 85, 1651–1664.

Toussaint, G., Burov, E., Jolivet, L., 2004. Continental plate collision: unstable versus stable dynamics. Geology 32, 33–36.

Turcotte, D.L., Schubert, G., 2002. Geodynamics. Cambridge University Press. 456 pp.

Von Blanckenburg, F., Davies, J.H., 1995. Slab breakoff: a model for syncollisional magmatism and tectonics in the Alps. Tectonics 14, 120–131.

Warren, C.J., Beaumont, C., Jamieson, R.A., 2008a. Modelling tectonic styles and ultra-high pressure (UHP) rock exhumation during the transition from oceanic subduction to continental collision. Earth Planet. Sci. Lett. doi:10.1016/j.epsl.2007.11.025.

Warren, C.J., Beaumont, C., Jamieson, R.A., 2008b. Formation and exhumation of ultra-high pressure rocks during continental collision: role of detachment in the subduction channel. Geochem. Geophys. Geosystems http://www.agu.org/journals/pip/gc/2007GC001839-pip.pdf.

Yamato, P., Agard, P., Burov, E., Le Pourhiet, L., Jolivet, L., Tiberi, C., 2007. Burial and exhumation in a subduction wedge: mutual constraints from thermomechanical modeling and natural *P–T–t* data (Sch. Lustrés, W. Alps). J. Geophys. Res. 112, B07410. doi:10.1029/2006JB004441.